Journal of Inflammation Research

Dovepress
open access to scientific and medical research

Open Access Full Text Article

ORIGINAL RESEARCH

Network Pharmacology and Experimental Validation of the Anti-Inflammatory Effect of Tingli Dazao Xiefei Decoction in Acute Lung Injury Treatment

Chengxi Zhang[1,2], Xiaoqian Li[1,2], Dan Gao[1,2], Huahe Zhu[3], Shun Wang[1,2], Bo Tan[4], Aidong Yang[1,2]

[1]School of Traditional Chinese Medicine, Shanghai University of Traditional Chinese Medicine, Shanghai, People's Republic of China; [2]Center for Traditional Chinese Medicine and Epidemic Disease, Shanghai Institute of Infectious Disease and Biosecurity, Shanghai, People's Republic of China; [3]Department of Integrative Medicine, Huashan Hospital, Fudan University, Shanghai, People's Republic of China; [4]Laboratory of Clinical Pharmacokinetics, Shuguang Hospital Affiliated to Shanghai University of Traditional Chinese Medicine, Shanghai, People's Republic of China

Correspondence: Aidong Yang; Bo Tan, Tel +86-21-135 6482 0109; +86-21-137 6418 9001, Fax +86-21-51322141; +86-21-20256699, Email aidongy@126.com; tbot@163.com

Purpose: Tingli Dazao Xiefei Decoction (TDXD) is a Traditional Chinese Medicine (TCM) formula used to treat acute lung injury (ALI). However, the precise mechanism of TDXD in treating ALI remains unclear. We investigated the therapeutic mechanism of TDXD against ALI using a complementary approach combining network pharmacology, molecular docking, and in vitro and in vivo experiments.

Material and Methods: Potential drug targets of TDXD and relevant target genes associated with ALI were retrieved from Chinese medicines and disease genes databases. Bioinformatics technology was employed to screen potential active ingredients and core targets. Validation experiments were conducted using a lipopolysaccharide (LPS)-induced ALI mouse (C57BL/6J) model, LPS-induced inflammatory RAW264.7 cells, and molecular docking between active compounds of TDXD and potential targets.

Results: Network pharmacology suggested that the mechanism of TDXD against ALI involved phosphoinositide 3-kinase (PI3K) / protein kinase B (AKT) / phosphatase and tensin homolog (PTEN) and Janus kinase 2 (JAK2) / signal transducer and activator of transcription 3 (STAT3) pathways. Quercetin, β-sitosterol, kaempferol, isorhamnetin, and L-stepholidine were identified as the main active compounds of TDXD that exerted anti-ALI effects. Molecular docking indicated that these compounds exhibited good binding capabilities (≤ −5kcal/mol) to key targets in PI3K/AKT/PTEN and JAK2/STAT3 signaling pathways. In the animal model, TDXD alleviated injuries and inflammatory responses in lung tissues, accompanied by inhibition of expression of tumor necrosis factor-α (TNF-α), Interleukin-6 (IL-6), STAT3, and Suppressor of Cytokine Signaling 3 (SOCS3) mRNA, and key proteins in PI3K/AKT/PTEN and JAK2/STAT3 pathways (all P values < 0.05). Cell based experiments showed that TDXD dose-dependently inhibited the expression of essential proteins in PI3K/AKT/PTEN and JAK2/STAT3 pathways ($P < 0.05$).

Conclusion: This study revealed that the mechanism of TDXD in ALI treatment might involve simultaneous regulation of PI3K/AKT/PTEN and JAK2/STAT3 pathways.

Keywords: network pharmacology, molecular docking, lipopolysaccharide, PI3K/AKT/PTEN, JAK2/STAT3

Introduction

Acute lung injury (ALI) is a clinical syndrome characterized by acute progressive respiratory distress and refractory hypoxemia. The main manifestations of ALI include increased alveolar-capillary membrane permeability, edema, and diffuse alveolar injury.[1] ALI can progress to acute respiratory distress syndrome (ARDS) and cause significant morbidity and mortality.[2,3] This is one of the critical reasons why patients are transferred to an intensive care unit and have a 40% fatality rate.[4] The pathogenesis of ALI/ARDS primarily includes pulmonary infection, pulmonary contusion, sepsis, etc.,

Received: 7 September 2023
Accepted: 12 December 2023
Published: 19 December 2023

among which infection is the most common cause.[5,6] Owing to the pathogenetic heterogeneity of ALI, effective treatments are lacking in clinical practice and adjuvant therapies, such as respiratory ventilation and symptomatic drugs, are typically used.[6,7] Therefore, there is an urgent need to thoroughly investigate the pathophysiologic mechanisms of ALI progression to identify improved prognostic and therapeutic targets. Studies have shown that inflammatory infiltration and hyperplasia of pulmonary microvascular endothelial cells induced by inflammatory factors, are essential pathogeneses of ALI.[8] Thus, inhibiting the activity of inflammatory effect can prevent and mitigate ALI/ARDS.

Traditional Chinese Medicine (TCM) has a long history of having unique advantages for treating various diseases, including ALI.[9] Tingli Dazao Xiefei Decoction (TDXD) is a TCM classical prescription treatment for lung diseases and consists of two herbs: Lepidii Semen Descurainiae Semen (Tinglizi) and Jujubae Fructus (Dazao). TDXD clears the lungs, promotes diuresis, relieves asthma, and promotes expectoration.[10] In addition, TDXD was found to significantly improve the prognosis of patients with ALI featuring severe pulmonary contusion by reducing the inflammatory response, shortening the respiratory rate, and improving the oxygenation index.[11] This TCM also effectively improves pulmonary symptoms and lung function in patients with pneumonia and reduces circulatory inflammation.[12] Consequently, TDXD is recommended by the administrative agency as one of the treatments for patients who are seriously ill with Coronavirus Disease-2019 (COVID-19).[13]

Herbal medicines usually have complex compositions and multiple targets, meaning their mechanisms of action can be difficult to understand.[14] Concordant with this observation, limited evidence has been provided to explain the mechanism underlying the therapeutic effect of TDXD. Recently, several studies have been conducted using a network pharmacology approach to determine the mechanism of action of TDXD in treating childhood pneumonia, COVID-19, and pulmonary heart disease.[15–17] However, without experimental validation in those studies, we can only speculate that the mechanism of action of TDXD in treating various diseases—including ALI might be related to the inhibition of inflammatory responses through several pathways, such as tumor necrosis factor (TNF), phosphoinositide 3-kinase/protein kinase B (PI3K-/AKT), etc. Consequently, the findings from such studies need to be further investigated and validated.

In the study, we integrated network pharmacology, molecular docking, and in vitro and in vivo studies to provide additional reliable evidence for elucidating the potential mechanism of TDXD in ALI treatment.

Materials and Methods

Drugs and Reagents

The TDXD granule used in the animal experiment was purchased from EFang Pharmaceutical Co., Ltd (Foshan, China). The TDXD used in vitro experiment was obtained from Shuguang Hospital, affiliated with Shanghai University of TCM. The lyophilized powder was prepared as follows: 45 g of Tinglizi (15 g) and Dazao (30 g) were decocted according to the method in the literature and then lyophilized, resulting in a powder with a 26.78% yield.[18] Dexamethasone (H37021969) was acquired from Cisen Pharmaceutical Co., Ltd. (Jining, China). Lipopolysaccharide (LPS) O55:B5 (L2880) was obtained from Merck (Darmstadt, Germany). Primary antibodies against (PI3K; 4249), protein kinase B (AKT; 4691), p-AKT (4060), phosphatase and tensin homolog (PTEN; 9188), signal transducer and activator of transcription 3 (STAT3; 12,640), p-STAT3 (9145), Janus kinase 2 (JAK2; 3230), p-JAK2 (4406), β-actin (4970) were obtained from Cell Signaling Technology (Boston, MA, USA). Protease and phosphatase inhibitor mixture (P1045), RIPA lysis buffer (P0013B), and a secondary antibody against rabbit IgG (A0208) were obtained from Beyotime Biotechnology (Shanghai, China). Sangon Biotech Co., Ltd (Shanghai, China) synthesized all primers used in the PCR experiment (see Supplementary Table S1 for primer details).

Collection of Drug Compounds and Related Targets

TCMSP, a database platform (https://tcmsp-e.com/tcmsp.php), and BATMAN-TCM, a bioinformatics analysis platform (http://bionet.ncpsb.org/batman-tcm/), were used to collect the chemical compounds and drug targets of two herbs in TDXD, Tinglizi, and Dazao, respectively.[19,20] Compounds were selected with the following criteria: oral bioavailability (OB) ≥ 30% and drug-likeness (DL) ≥ 0.18 or score cutoff (≥ 20 points). Subsequently, the selected compounds were evaluated as potential active compounds of TDXD.

Collection of Disease Targets

The keywords "acute lung injury" and "acute respiratory distress syndrome" were used to search four databases: GeneCards (https://www.genecards.org/), DisGeNET (https://www.disgenet.org/), TTD (https://db.idrblab.net/ttd/), and CTD database (https://ctdbase.org/), respectively. All targets of diseases related to ALI were collected and duplicates were removed. Subsequently, the Wayne diagram (http://www.bioinformatics.com.cn/) was applied to identify the intersection of drug-related targets and disease-related targets. Overlapping targets were considered candidate key targets for TDXD in ALI treatment.

Screening of Core Targets by Protein–Protein Interaction Network

The STRING database (https://string-db.org/) generated a protein-protein interaction (PPI) network filtered by a PPI score > 0.9 with hidden disconnected nodes removed. Cytoscape (v3.9.0) was used to visualize and analyze the selected targets. The significance of network nodes was assessed through a two-step screening process using six topological parameters: Degree Centrality, Betweenness Centrality, Closeness Centrality, Eigenvector Centrality, Network Centrality, and Local average connectivity-based method. The criteria are identical in the two-processes steps, and any targets with values of topological parameters above or equal to the median remain.[17]

Enrichment Analyses

Using the Database for Annotation, Visualization and Integrated Discovery (DAVID, https://david.ncifcrf.gov/), the potential core targets were subjected to Kyoto Encyclopedia of Genes and Genome (KEGG) pathway and Gene Ontology (GO) enrichment analyses. Twenty representative signaling pathways from KEGG analysis and the top 10 signaling pathways from GO analysis, including biological processes, cell components, and molecular functions, were selected based on their P-values set at $P < 0.05$.

Construction of "Herb-Compound-Target-Pathway" Network

Cytoscape (v3.9.0) created a herbs-compound-target-signaling pathway network using potential active compounds, core targets, and related signaling pathways. Topological parameters of active compounds corresponding to core targets were analyzed using the Analyze Network function of Cytoscape (v3.9.0). The top 5 compounds, ranked by degree values, were identified as the essential compounds of TDXD in ALI treatment.

Molecular Docking

The RCSB Protein Data Bank database (http://www.rcsb.org/) was used to obtain the molecular structures of six core targets. Meanwhile, the PubChem database (https://pubchem.ncbi.nlm.nih.gov/) was used to obtain the molecular structures of the potential active compounds of TDXD and the positive control, dexamethasone. These targets and compound molecules were pretreated with PyMOL (v2.5.4) and ADFR (v1.0), respectively. Subsequently, molecular docking simulations were performed using SailVina (v1.0) to extract the minimum binding energy for molecular docking. The binding energy numerical value reflects the magnitude of the binding ability and interaction between molecules. Binding energy < 0 kcal/mol usually indicates spontaneous ligand receptor protein binding, and a binding energy < −1.2 kcal/mol indicates good binding capacity. The best-bound set of molecular docking results for each group was visualized using PyMOL (v2.5.4).

Animal Experiment

Fifty male C57BL/6J mice aged 6–8 weeks and weighing 18–20 g were purchased from Shanghai Sippe-Bk Lab Animal Co., Ltd. (Shanghai, China). The mice were assigned to one of five groups at random: normal (normal saline), model (LPS), low-dose of TDXD (5.85 g/kg), high-dose TDXD (11.7 g/kg), and dexamethasone (Dex) (5 mg/kg), with 10 mice in each group. After one week of adaptive feeding, the corresponding solution in each group was administered once daily for six consecutive days. On day 7, at 2 hours after administration, the ALI model was stimulated by intraperitoneal injection of LPS (2 mg/mL) in all groups except the normal group. Samples were taken 8 h after ALI modeling. The daily therapeutic dose of TDXD is approximately 45 g of raw drug per person (70 kg),[21] and the equivalent dose for the mouse was calculated as 5.85 g/kg using the body surface area method.[22] Accordingly, the TDXD dosages in the studies were selected as 5.85 and 11.7 g/kg (two folders of equivalent human dose) for low-dose and high-dose groups, respectively, which are equivalent as those used in rat studies.[23,24]

All mice were kept under a SPF-level barrier system (License No.: SCXK (Shanghai) 2018–0006; Shanghai Laboratory Animal Quality Certificate: 20180006038718) at the Animal Laboratory Center of Shanghai University of TCM, with suitable temperature (25–27°C) and humidity (40–60%). All mice were fed water and a chow diet ad libitum before the experiments. The animal experiment was approved by the Experimental Animal Welfare and Ethics Committee of Shanghai University of Traditional Chinese Medicine (Ethics No.: PZSHUTCM220613025). The experiments were conducted in strict adherence to the guidelines outlined in the Care and Use of Laboratory Animals of the National Institutes of Health for animal experiments.

Hematoxylin–Eosin Staining for Pathological Changes

Hematoxylin-eosin (HE) staining was used to detect pathological changes in lung tissues. The left lung of each mouse was fixed for 24 h in 4% paraformaldehyde. Next, the fixed tissues were dehydrated in alcohol, rendered transparent, and embedded in wax. The implanted samples were then cut into paraffin blocks and dewaxed. Pathological changes in lung tissues were observed using a light microscope with a magnification of 200x.

Enzyme-Linked Immunosorbent Assay

Mouse bronchoalveolar lavage fluid (BALF) was collected according to reported procedures. The withdrawn fluid was centrifuged at 3000 rpm for 10 min at 4°C. The contents of inflammatory factors such as IL-1β, IL-6, and TNF-α in mouse alveolar lavage fluid were measured by respective enzyme-linked immunosorbent assay (ELISA) kits (Wei-Ao Biotechnology Co., Ltd., Shanghai, China) according to the manufacturer's instruction manuals. The ELISA plates were read with a microplate reader (BioTek, Winooski, VT) at 450 nm.

CCK-8 Assay

Mouse mononuclear macrophage RAW264.7 cells were purchased from the National Collection of Authenticated Cell Cultures (Shanghai, China). The cells were cultured in Dulbecco's Modified Eagle Medium (DMEM) containing fetal bovine serum and 10% penicillin-streptomycin in a CO2 incubator at 37°C. RAW264.7 cells in logarithmic growth phase were inoculated into a 96-well plate for 24 h before treating with different concentrations (0, 50, 100, 200, 400, 600, 800, 1600, and 3200 μg/mL) of TDXD solution. Cell proliferation was determined by CCK-8 assay (Beyotime Biotechnology Co., Ltd., Shanghai, China) according to the instruction manual. Using a Benchmark microplate reader (Bio-Rad, Hercules, CA, USA), the absorbance value of each well was measured at 450 nm. Subsequently, in further experiments, TDXD concentrations of 400, 600, and 800 μg/mL were used for low-, medium-, and high-dose groups, respectively.

Cell Culture

RAW264.7 cells (2×10^5 cells/mL) were inoculated into 6-well plates. The cells were classified as follows: normal group, model group, and TDXD (low, medium, and high doses) groups, and triplicate wells were set up in each group. When the cell confluence reached 80%–90%, blank culture medium, LPS (1 μg/mL), and different doses of lyophilized powder solution of TDXD (400, 600, and 800 μg/mL) were added to the appropriate wells. After incubation for 24 h, the culture medium was discarded. The cells were then washed with PBS, collected, and observed under a BH2 microscope (Olympus, Japan).

Real-Time PCR

IL-1β, IL-6, TNF-α, STAT3, and SOCS3 mRNA expression levels in mouse lung tissues and RAW264.7 cells were determined using real-time PCR (RT-PCR) analysis. Briefly, RNA was extracted from lung tissue and cell samples according to the instructions of the EZB Kit (RN001-plus, Yingze Biomedical Technology Co., Ltd., Suzhou, China) and reverse-transcribed to cDNA with a RT kit (RR036A, TAKARA, Tokyo, Japan) following the instructions of the kit. RT-PCR experiments were then conducted by using a TB Green Kit (RR420A, TAKARA, Tokyo, Japan) with a LightCycler96 instrument (Roche, Switzerland). The respective gene expressions were calculated by the $2^{-\Delta\Delta CT}$ method.[25] The primer sequences are exhibited in the Supplementary Material-S1.

Western Blotting

Protein expression levels of PI3K, p-AKT, AKT, PTEN, p-STAT3, STAT3, p-JAK2, and JAK2 in mouse lung tissues and RAW264.7 cells were detected using Western blotting. Briefly, the protein concentration of homogenized samples from mouse lung tissues or RAW264.7 cells was quantified using a BCA kit (ZJ102, Epizyme Biotech Co., LTD., Shanghai, China) according to the manufacturer's instructions.[26] Protein samples were then subjected to sodium dodecyl sulfate-polyacrylamide gel electrophoresis (SDS-PAGE). After the processes of electrophoresis, transfer to polyvinylidene fluoride (PVDF) membranes, and blockage, the corresponding primary antibody was incubated with the sample overnight at 4°C. The secondary antibody was then incubated at ambient temperature for 1 h. Proteins were visualized using a Bio-Rad imaging system and an ECL chemiluminescence kit (P0018FM, Beyotime). ImageJ (v1.47, NIH) software was used to examine grayscale values.

Statistical Methods

Experimental data were presented as mean ± standard deviation. GraphPad Prism software (v8.0.2, GraphPad, San Diego, CA) was used for statistical analysis. One-way analysis of variance (ANOVA) was employed to compare multiple groups, and Tukey's test was used for comparisons between two groups. $P < 0.05$ was considered statistically significant.

Results

Potential Active Compounds and Targets of TDXD for the Treatment of ALI

Based on the TCMSP and BATMAN-TCM databases,13 potentially active compounds of Tinglizi and 55 potentially active compounds of Dazao were identified (Figure 1A and Supplementary Table S2). Furthermore, 104 drug targets for Tinglizi

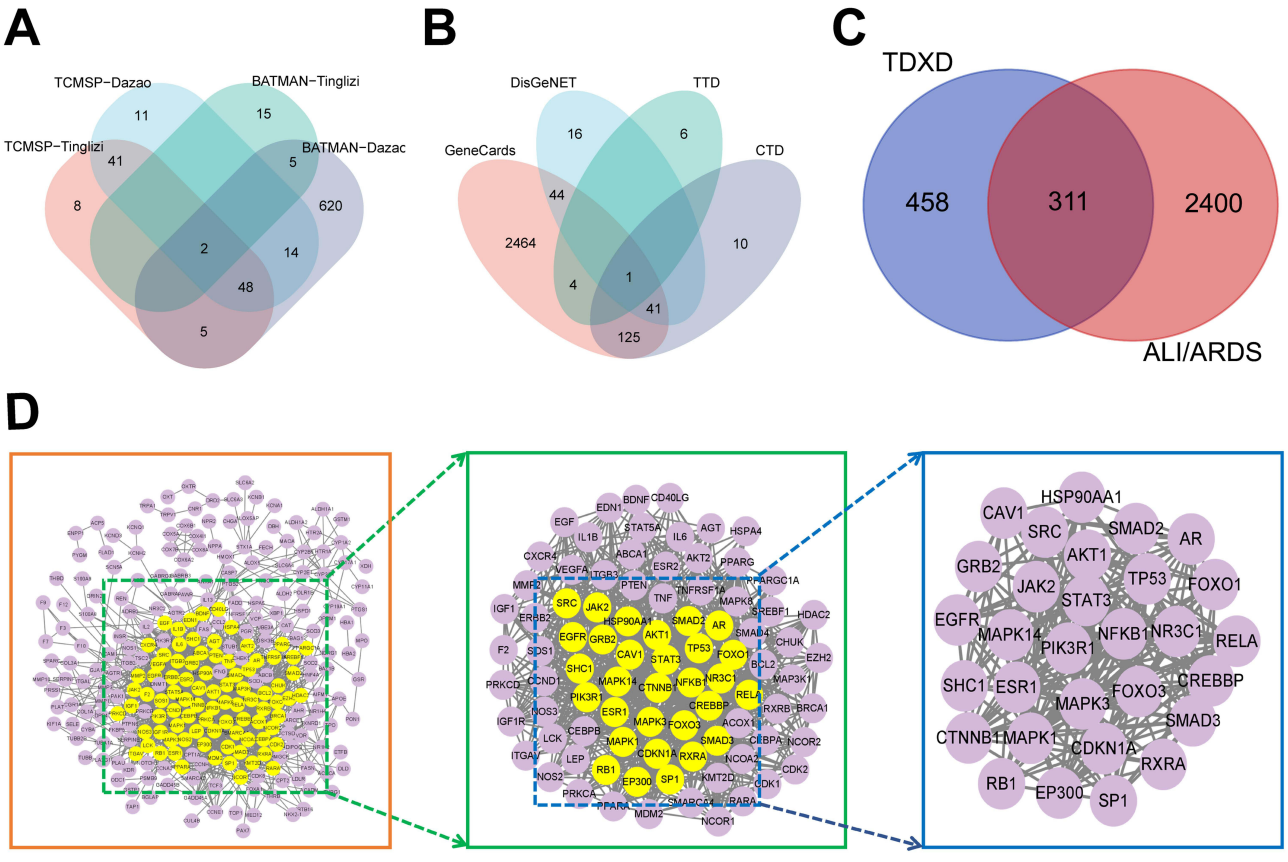

Figure 1 Screening of potential targets and core targets of TDXD for the treatment of ALI. (**A**) Venn diagram of potential targets of TDXD. (**B**) Venn diagram of potential targets of ALI disease. (**C**) Venn diagram of intersection of drug targets and disease-related targets. (**D**) PPI network diagram of potential targets and core target screening results of TDXD in the treatment of ALI.

and 116 drug targets for Dazao were obtained from the TCMSP database, as well as 22 drug targets for Tinglizi and 694 drug targets for Dazao from the BATMAN-TCM database. After removing duplicates, 769 drug-related targets remained (Supplementary Table S3). Using GeneCards, DisGeNET, TTD, and CTD databases, 2679, 102, 11, and 177 targets connected to ALI-related diseases were obtained, respectively. After removing duplicates, 2711 targets associated with ALI-related diseases were obtained (Figure 1B and Supplementary Table S4). Based on the overlap of drug and disease-related targets, 311 potential targets of TDXD for the therapy of ALI were identified (Figure 1C and Supplementary Table S5).

PPI Network Establishment and Core Targets Identification

A PPI network was established with the STRING database. First, the corresponding data were imported into Cytoscape, then, the CytoNCA plugin was used to conduct a two-step process to screen core targets. In the first step, the topological parameters' median of ≥ 6 (6, 74.1183, 0.05025314, 0.018699061, 2.8, 3.6, respectively) was employed as the screening criterion, which yielded 87 targets. In the second step, the same median value (≥ 6) of the topological parameters (19, 30.619884, 0.5408805, 0.08889559, 8.1, 9.917892, respectively) was used, resulting in the identification of 30 targets as core targets (Figure 1D and Supplementary Table S6).

KEGG and GO Enrichment Analyses

KEGG analysis for the core targets revealed several closely associated signaling pathways, including the chemokine signaling pathway, pathways regulating pluripotency of stem cells, the PI3K-AKT signaling pathway, the shigellosis signaling pathway, and the JAK-STAT signaling pathway (Figure 2A). Among these pathways, the PI3K/AKT/PTEN and JAK2/STAT3 signaling pathways were highly ranked; thus, we focused on these pathways and their key molecules, such as AKT, STAT3, IL-6, PTEN, PIK3R1, and JAK2.

The GO enrichment analysis (Figure 2B) revealed that the core targets were closely associated with several biological processes, including negative regulation of RNA polymerase II gene promoter transcription, positive regulation of protein entry into the nucleus, and positive regulation of pre-miRNA transcription. In addition, the cellular compounds most closely associated with these targets were integrative transcription factors, chromatin, and membrane rafts. The molecular functions most closely associated with the targets were sequence-specific DNA binding in transcriptional regulatory regions, transcription factor binding, and RNA polymerase II transcription factor activity.

The Network of "Herb-Compound-Target-Pathway" and Key Active Compounds

We used the primary targets, probable active compounds of TDXD, and the related signaling pathways to construct a herb-compound-target-pathway network (Figure 3). Topological analysis showed that the five compounds with the highest degree values were MOL000098 (quercetin), MOL000358 (β-sitosterol), MOL000422 (kaempferol), MOL000354 (isorhamnetin), and MOL000627 (L-stepholidine), respectively (Supplementary Table S7).

Molecular Docking Validation

Molecular docking analysis was performed between the potential active compounds including quercetin, β-sitosterol, kaempferol, isorhamnetin, and L-stepholidine, and the six core targets AKT1 (PDB: 3CQU), STAT3 (PDB: 6GFA), IL-6 (PDB: 2L3Y), PTEN (PDB: 1D5R), PIK3R1 (PDB: 4OVV), and JAK2 (PDB: 2B7A). Dexamethasone was also used as a positive control. All five active compounds and dexamethasone had good binding affinity with the protein targets (Table 1). Among the compounds, quercetin had the highest affinity for AKT1 and STAT3, β-sitosterol had the highest affinity for IL-6, dexamethasone had the highest affinity for PTEN, quercetin had the highest affinity for PIK3R1, and kaempferol had the highest affinity for JAK2. The binding interaction patterns of each pair of molecules and targets are shown in Figure 4.

Experimental Validation

Following intraperitoneal injection of LPS, HE staining of mouse lung tissues revealed interstitial pneumonia and edema around small blood vessels in the lung. This lung injury was improved with TDXD, with the most significant improvement observed in the TDXD high-dose group (Figure 5A). The ELISA results showed that the levels of

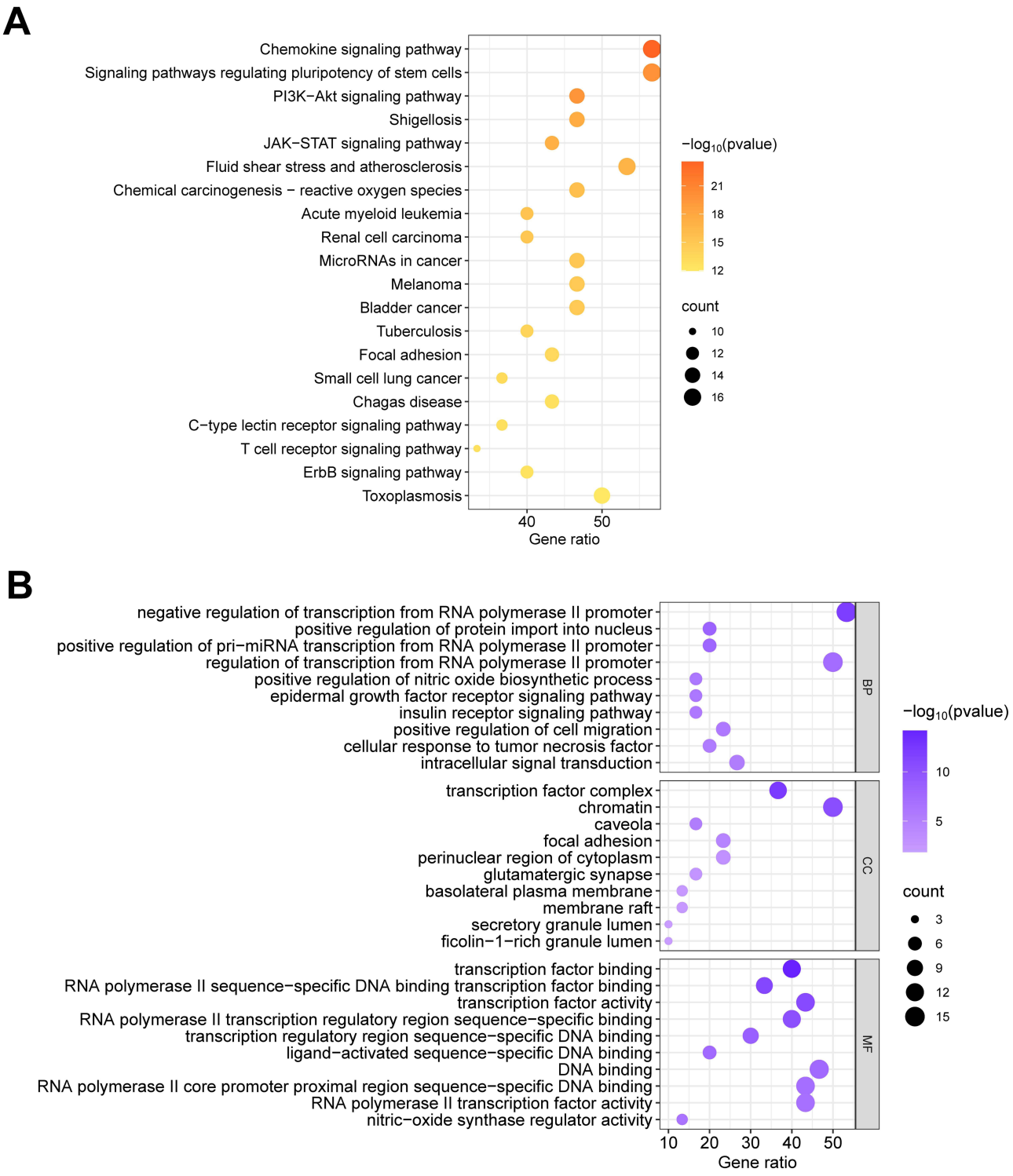

Figure 2 Enrichment analysis and drug-compound-target-pathway network diagram. (**A**) KEGG pathway enrichment bubble diagram. (**B**) GO enrichment analysis bubble diagram.

Abbreviations: BP, biological process; CC, cellular components; MF, molecular function.

inflammatory cytokines IL-1β, IL-6, and TNF-α in mouse BALF increased after the administration of LPS ($P < 0.01$). However, after the administration of TDXD, the levels of these inflammatory factors were reduced ($P < 0.05$), with the most significant reduction detected in the high-dosage group (Figure 5B).

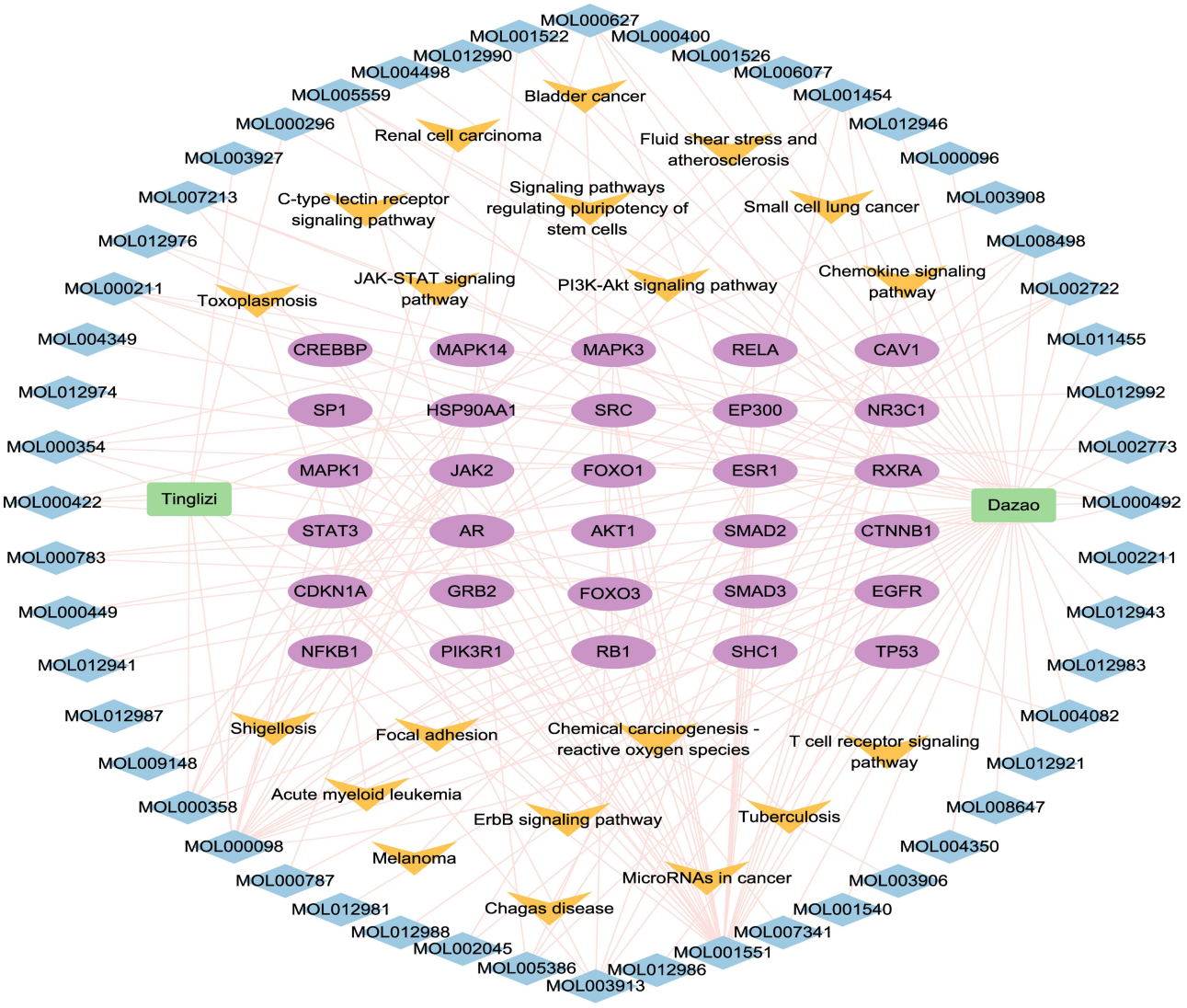

Figure 3 Drug-compound-target-pathway network diagram. Green rectangles represent traditional Chinese medicines, blue diamonds represent active ingredients, purple ovals represent core targets, yellow inverted triangles represent signaling pathways.

The qPCR experiments demonstrated that IL-6, TNF-α, STAT3, and SOCS3 mRNA expression in mouse lung tissues was significantly elevated after intraperitoneal injection of LPS ($P < 0.01$) (Figure 6A). Conversely, administration of TDXD reduced the expression of IL-6, TNF-α, STAT3, and SOCS3 mRNA ($P < 0.01$), with the

Table 1 Docking and Binding Capability of Five Potential Active Compounds to Each Core Target Protein (Kcal/Mol)

	AKT1	STAT3	IL-6	PTEN	PIK3R1	JAK2
Quercetin	−9.5*	−9.3*	−7.9	−7.7	−6.5*	−8.9
β-sitosterol	−5.1	−8.2	−8.6*	−7.2	−5.9	−6.7
Kaempferol	−9.3	−8.9	−8.1	−7.6	−6.2	−9.0*
Isorhamnetin	−9.4	−9.2	−7.6	−7.6	−6.1	−9.0
Stepholidine	−8.0	−8.8	−8.5	−7.9	−6.3	−8.7
Dexamethasone	−5.0	−9.3	−7.4	−8.2*	−6.2	−5.9

Notes: *Indicates an active compound that has the optimal binding capability for each core target protein.

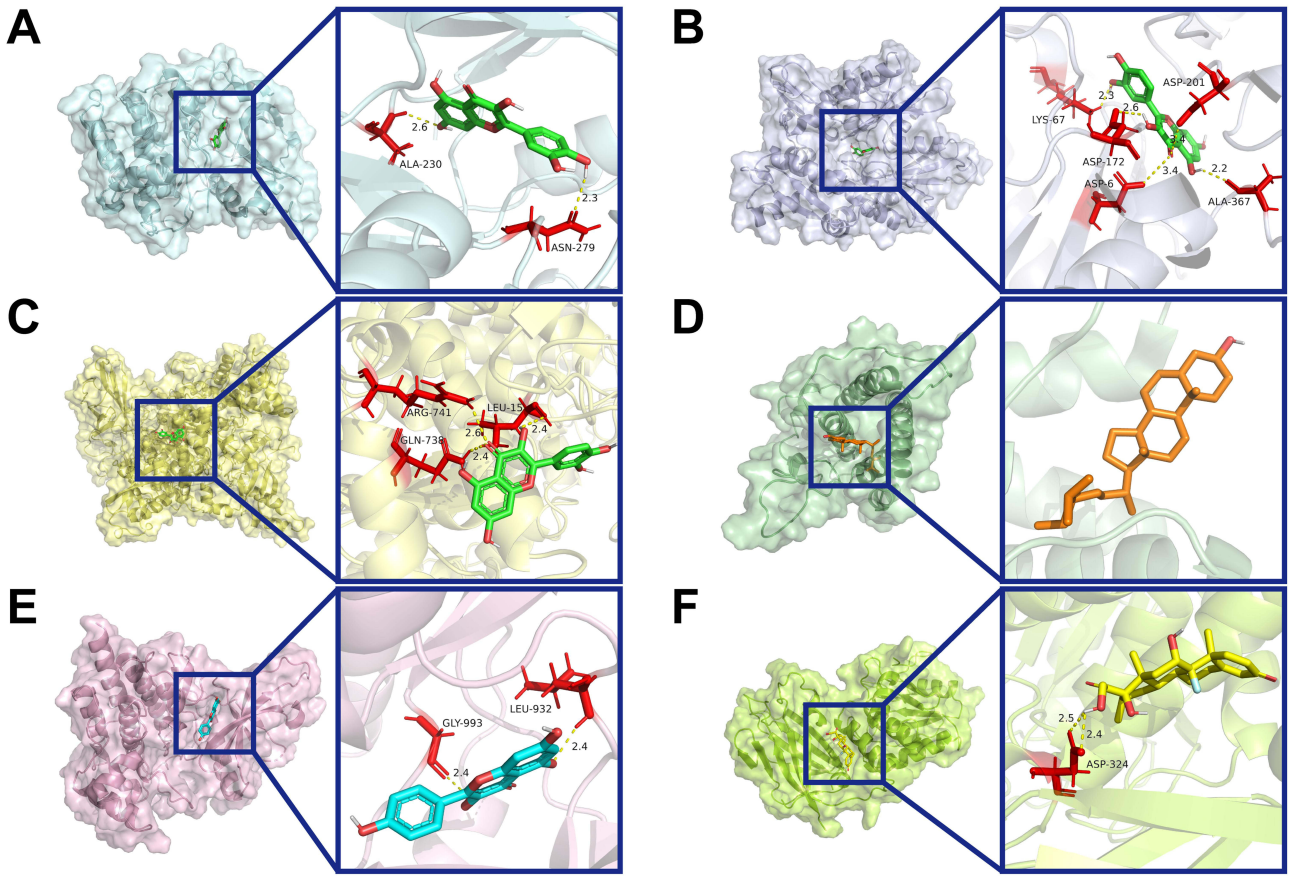

Figure 4 Representative docking pattern between six core targets and their optimal binding active compounds. (**A**) AKT1 and quercetin; (**B**) STAT3 and quercetin; (**C**) IL-6 and β-sitosterol; (**D**) PTEN and dexamethasone; (**E**) PIK3R1 and quercetin; (**F**) JAK2 and kaempferol.

most significant reduction observed at high doses. Additionally, Western blot analysis showed a decrease in PTEN protein expression ($P < 0.05$), and increases in PI3K, p-AKT/AKT, p-STAT3/STAT3, and p-JAK2/JAK2 protein expression or the protein expression ratio ($P < 0.05$) in lung tissues of ALI model mice. Furthermore, administration of TDXD increased PTEN protein expression while decreasing PI3K, p-Akt/AKT, p-STAT3/STAT3, and p-Jak2/JAK2 protein expression or the ratio of protein expression ($P < 0.05$) (Figure 6B). These findings suggested that TDXD might alleviate LPS-induced lung inflammation and lung injury in mice by down-regulating PI3K/AKT/PTEN and JAK2/STAT3 signaling pathways.

In the CCK-8 assay, the lyophilized powder of TDXD did not have a significant inhibitory effect on cells at concentrations ranging from 0 to 1600 μg/mL. Therefore, concentrations of 400, 600, and 800 μg/mL were selected as the concentrations administered to low-, medium-, and high-dose groups for cellular experiments (Figure 7A). The qPCR results indicated that IL-1β, IL-6, and TNF-α mRNA expression increased in cells following LPS administration ($P < 0.01$). Conversely, the administration of TDXD lowered the expression of IL-1β, IL-6, and TNF-α mRNA in RAW264.7 cells ($P < 0.05$) in a dose-dependent manner (Figure 7B). Additionally, Western blot analysis revealed that macrophage PI3K, p-AKT/AKT, p-STAT3/STAT3, and p-JAK2/JAK2 protein levels or protein levels ratio increased ($P < 0.05$), and PTEN protein levels decreased ($P < 0.05$) following LPS administration. In contrast, PI3K, p-AKT/AKT, p-STAT3/STAT3, and p-JAK2/JAK2 protein expression or the ratio of protein expression decreased ($P < 0.05$), and PTEN protein expression increased ($P < 0.05$) in all groups of cells following the administration of TDXD (Figure 7C). These findings showed that TDXD might alleviate LPS-induced inflammatory responses in macrophages by down-regulating PI3K/AKT/PTEN and JAK2/STAT3 signaling pathways.

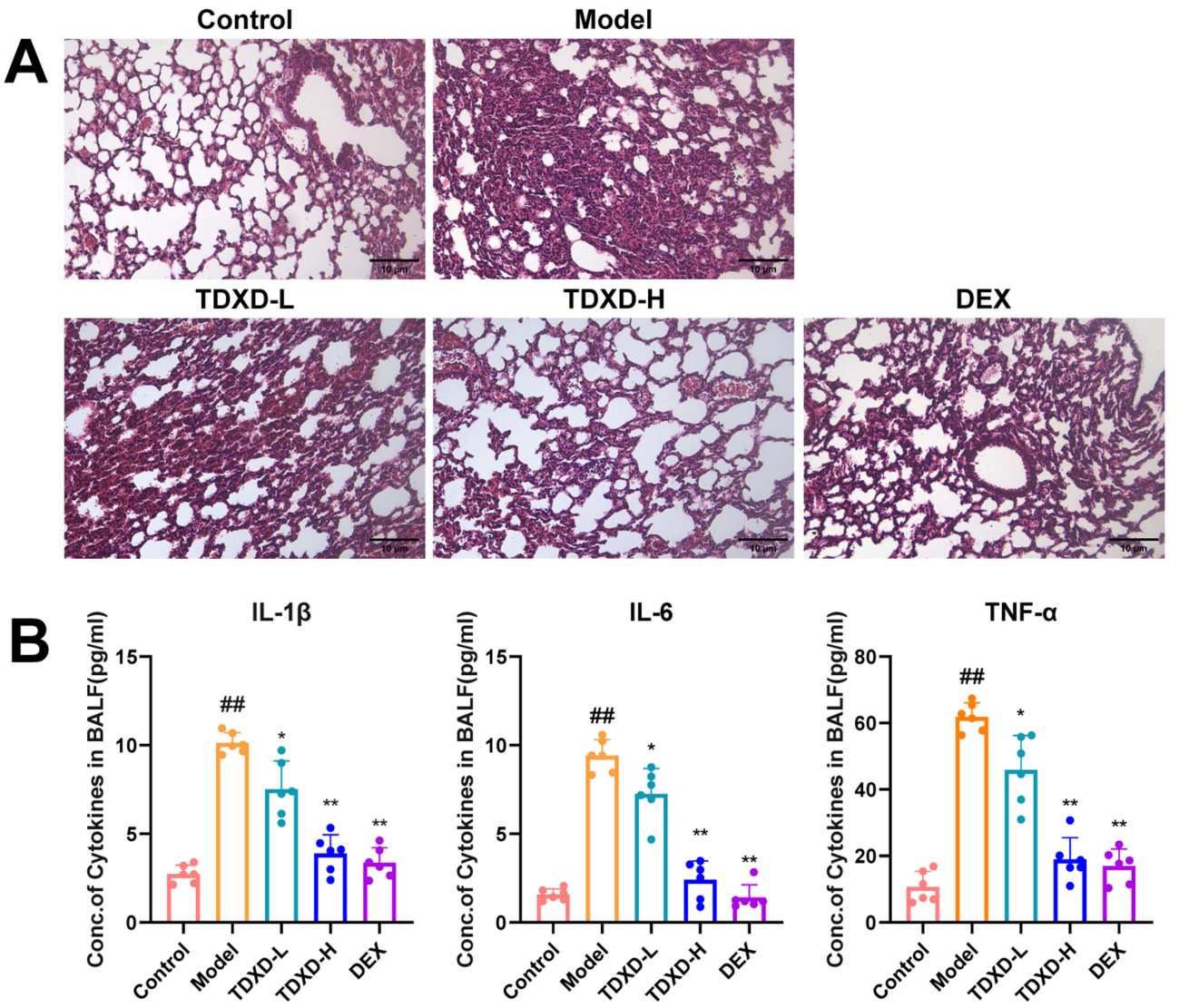

Figure 5 Anti-inflammatory effects of TDXD on LPS-induced mice. (**A**) Histomorphology of mice lungs (HE-stained, ×200). (**B**) Pro-inflammatory factors IL-1β, IL-6, and TNF-α in alveolar lavage fluid analyzed by ELISA (mean ± SD, n = 6). ##P < 0.01, compared with normal group;*P < 0.05 and **P < 0.01, compared with model group.

Discussion

TDXD is a TCM formula commonly applied for treating respiratory diseases, such as pneumoconiosis, bronchopneumonia, mycoplasma pneumonia, and bronchial asthma.[27–30] In patients with ALI, TDXD could effectively reduce the inflammatory response, shorten the duration of mechanical ventilation, and improve the curative ratio.[31] Utilizing a single network pharmacology approach, researchers have predicted potential mechanisms for TDXD treatment in childhood pneumonia, conjunctivitis, and pulmonary heart disease.[15–17] Several targets and signaling pathways, including TNF, PI3K-AKT, and other inflammatory pathways, are suggested to be highly relevant. However, to our knowledge, these findings have not been experimentally validated. Therefore, a comprehensive study that integrated multiple dimensions on the mechanism of TDXD treatment in ALI would be benefit for the clinical application of the TCM formula. Thus, in this study, we investigated the mechanism of TDXD for ALI treatment using an integrated approach that combined network pharmacology and experimental validation, namely animal, cellular, and molecular docking experiments.

Potential drug targets and disease-related targets were obtained from several public databases. A network pharmacological approach, was used to screen the core targets and major active compounds, and further KEGG and GO enrichment analyses indicated that the mechanism of TDXD for ALI treatment might be highly related to several

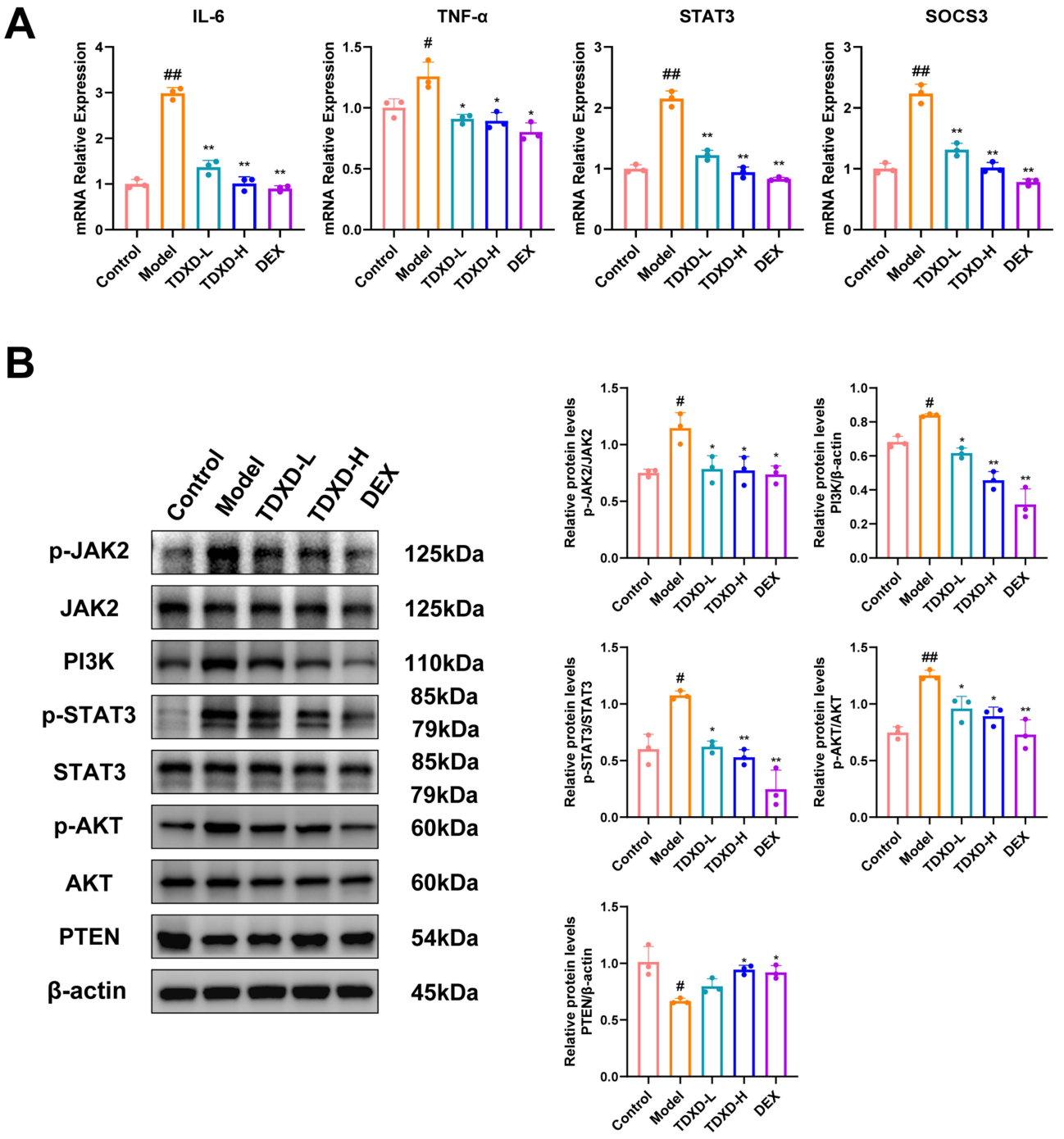

Figure 6 TDXD inhibited PI3K/AKT/PTEN and JAK2/STAT3 signaling pathways in LPS-induced mice. (**A**) mRNA expression of IL-6, TNF-α, STAT3, and SOCS3 in mice lung tissues analyzed by RT-PCR (mean ± SD, n = 3). (**B**) Protein expression of PI3K, p-AKT/AKT, PTEN, p-STAT3/STAT3, and p-JAK2/JAK2 analyzed by Western blotting (mean ± SD, n = 3). Each experiment was conducted in triplicate. $^{\#}P < 0.05$ and $^{\#\#}P < 0.01$, compared with normal group; $^{*}P < 0.05$ and $^{**}P < 0.01$, compared with model group.

signaling pathways, for example, PI3K/AKT/PTEN and JAK2/STAT3 pathways. Subsequently, we conducted validation experiments in C57BL/6J mice and RAW264.7 macrophages, demonstrating that TDXD could significantly inhibit LPS-induced inflammation by simultaneously regulating PI3K/AKT/PTEN and JAK2/STAT3 signaling pathways. For example, in the mouse experiment, TDXD attenuated lung pathological injury and the expression of pro-inflammatory factors (IL-1β, IL-6, and TNF-α) accompanied by down-regulation of PI3K, p-AKT, p-STAT3, and p-JAK2 expression.

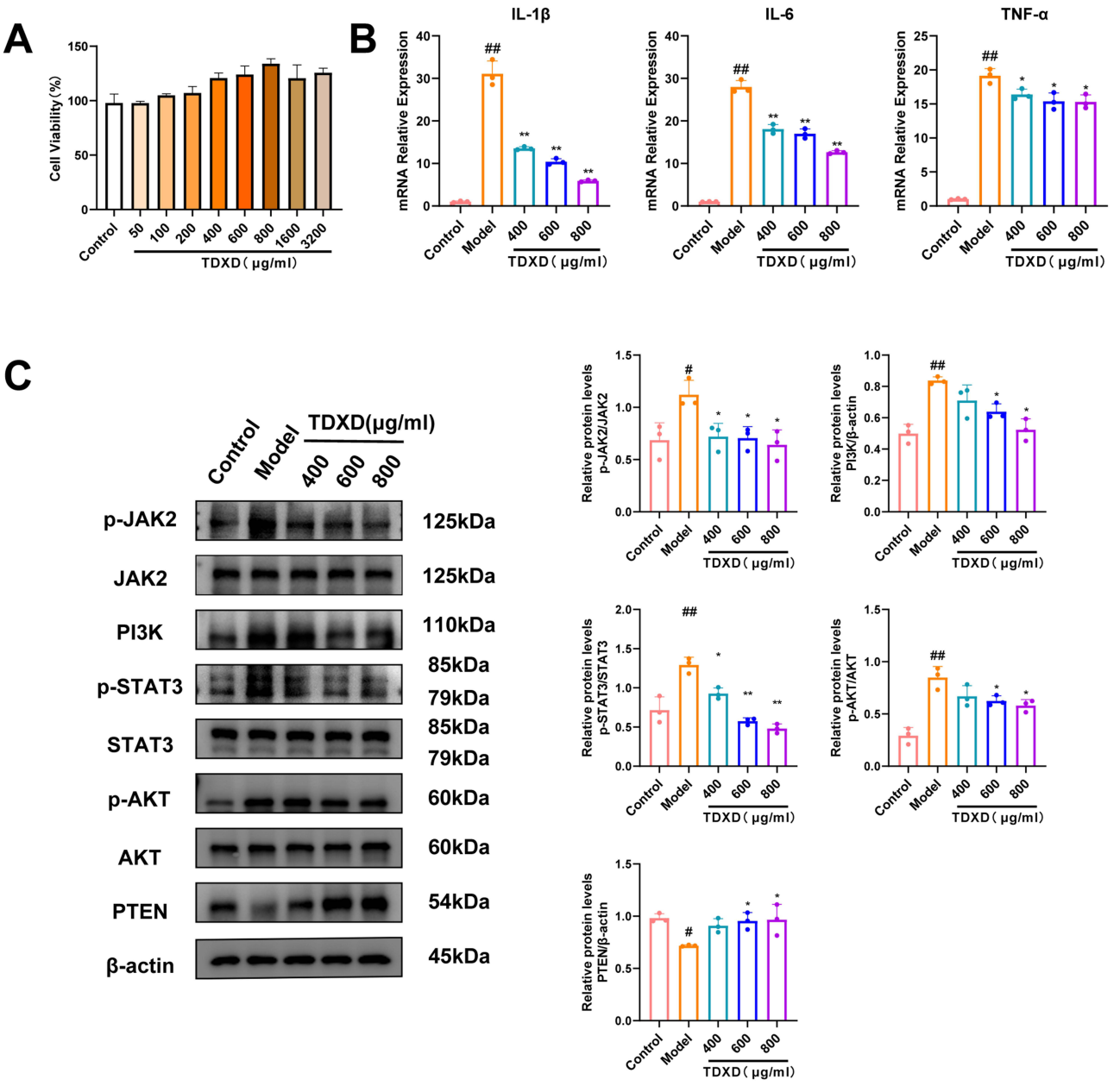

Figure 7 TDXD attenuated inflammatory responses related to inhibition of PI3K/AKT/PTEN and JAK2/STAT3 signaling pathways in LPS-induced RAW264.7 cells. (**A**) Cell viability analyzed by CCK-8 (mean ± SD, n = 3). (**B**) mRNA expression of IL-1β, IL-6, and TNF-α analyzed by RT-PCR (mean ± SD, n = 3). (**C**) Protein expression of PI3K, p-AKT/AKT, PTEN, p-STAT3/STAT3, and p-JAK2/JAK2 analyzed by Western blotting (mean ± SD, n = 3). Each experiment was conducted in triplicates. $^{\#}P < 0.05$ and $^{\#\#}P < 0.01$, compared with normal group; $^{*}P < 0.05$ and $^{**}P < 0.01$, compared with model group.

Similarly, in the cellular experiments, TDXD simultaneously decreased protein expression of PI3K, p-AKT, p-STAT3, and p-JAK2 in a dose-dependent manner.

JAK2/STAT3 and PI3K/AKT/PTEN signaling pathways are closely associated with ALI pathogenesis. The JAK/STAT3 pathway is a non-receptor-type tyrosine-protein kinase/signaling and activator of transcription 3 pathway that is stimulated by IL-6. Upon cytokine stimulation, JAK2/STAT3 signaling is activated, resulting in increased phosphorylation of downstream protein phosphatase (SHP2), upregulation of transcription target protein SOCS3, and activation of pro-inflammatory factors, which induce ALI.[32] Phosphorylation of JAK2 and STAT3 is significantly increased in rat models of ALI.[33,34] Inhibiting the JAK2/STAT3 pathway may protect the lungs by preventing release of members of the interleukin family. Similarly, the PI3K/AKT pathway is instrumental in the development of ALI and can be intervened by

regulating mitochondrial function, oxidative stress, and inflammatory responses. PTEN inhibits AKT activity by dephosphorylating PIP3.[35] Previous research showed that downregulating PI3K/AKT pathway could protect against LPS-induced ALI.[36]

To validate five potential active compounds of TDXD (quercetin, β-sitosterol, kaempferol, isorhamnetin, and L-stepholidine), which were identified in the network pharmacological screening, a molecular docking model was constructed using six key target proteins, namely AKT1, STAT3, IL-6, PTEN, PIK3R1, and JAK2. The results showed that the five potential active compounds had a high affinity for the key targets, especially AKT1, STAT3, PIK3R1, and JAK2. Previous studies support the role of these five compounds in the treatment of ALI. For example, quercetin functions as an anti-inflammatory and antioxidant in ALI therapy by lowering levels of pro-inflammatory cytokines (IL-6 and TNF-α), decreasing MDA expression, increasing T-SOD production, and decreasing apoptosis.[37] Intervention with β-sitosterol in the LPS-induced RAW264.7 inflammatory model significantly alleviate ALI by activating the LXRs/ABCA1 pathway.[38] Kaempferol has antioxidant and anti-inflammatory properties that could effectively alleviate virus-induced ALI by inhibiting the TLR4/MyD88-mediated NF-kB and MAPK pathways.[39] In addition, both isorhamnetin and L-stepholidine exhibited high affinities with the key targets in our molecular docking experiment, suggesting that they would be active compounds of TDXD for ALI treatment, and this which needs further investigation.

Conclusion

Using an integrated approach involving with network pharmacology, and animal, cellular, and molecular docking studies, we found that TDXD could attenuate excessive lung inflammation by simultaneously inhibiting PI3K/AKT/PTEN and JAK2/STAT3 signaling pathways, thereby reducing the severity of ALI. In addition, we found five active compounds of TDXD including quercetin, β-sitosterol, kaempferol, isorhamnetin, and L-stepholidine might be responsible for the anti-inflammatory effects of TDXD.

Abbreviations

AKT, Protein kinase B; ALI, acute lung injury; ARDS, acute respiratory distress syndrome; BALF, bronchoalveolar lavage fluid; BATMAN-TCM, Bioinformatics Analysis Tool for Molecular mechANism of Traditional Chinese Medicine; BC, Betweenness Centrality; CC, Closeness Centrality; COVID-19, Coronavirus Disease-2019; DAVID, Database for Annotation, Visualization, and Integrated Discovery; DC, Degree Centrality; Dex, dexamethasone; DL, drug-likeness; DMEM, Dulbecco's Modified Eagle Medium; EC, Eigenvector Centrality; GO, Gene Ontology; HE, Hematoxylin–Eosin staining; IL, Interleukin; JAK2, Janus kinase 2; KEGG, Kyoto Encyclopedia of Genes and Genome; LAC, Local average connectivity-based method; LPS, Lipopolysaccharide; NC, Network Centrality; OB, oral bioavailability; PI3K, phosphoinositide 3-kinase; PPI, protein–protein interaction; PTEN, Phosphatase and tensin homolog; RCSBPDB, RCSB Protein Data Bank; STAT3, Signal transducer and activator of transcription 3; SOCS3, Suppressor of Cytokine Signaling 3; TCMSP, TCM, Systems Pharmacology Database; TDXD, Tingli Dazao Xiefei Decoction; TNF, tumor necrosis factor.

Acknowledgments

All the authors of this manuscript are thankful to their respective Departments/Universities for the successful completion of the study.

Funding

This work was supported by the Shanghai Municipal Science and Technology Major Project (ZD2021CY001, ZXS004R4-1), the National Natural Science Foundation of China (81673855), the Shanghai University of Traditional Chinese Medicine Budget Project (2021LK075), and by the Shanghai Shuguang Hospital Siming Project (SGXZ-201907).

Disclosure

The authors report no conflicts of interest in this work.

References

1. Yasmeen B, Anna K, Craig AT. Acute lung injury a clinical and molecular review. *Arch Pathol Lab Med*. 2016;140(4):345–350. doi:10.5858/arpa.2015-0519-RA
2. Erickson SE, Martin GS, Davis JL, Matthay MA, Eisner MD. Recent trends in acute lung injury mortality: 1996–2005. *Crit Care Med*. 2009;37(5):1574–1579. doi:10.1097/CCM.0b013e31819fefdf
3. Antoine M, Yinggang Z, Varun G, Hyungsun L, Lee JW. Mesenchymal stem cell derived secretome and extracellular vesicles for acute lung injury and other inflammatory lung diseases. *Expert Opin Biol Ther*. 2016;16(7):859–871. doi:10.1517/14712598.2016.1170804
4. Bellani G, Laffey JG, Pham T, et al. Epidemiology, patterns of care, and mortality for patients with acute respiratory distress syndrome in intensive care units in 50 countries. *JAMA*. 2016;315(8):788–800. doi:10.1001/jama.2016.0291
5. Chyun SC, Gong MN, Hong ZR, et al. The influence of infection sites on development and mortality of ARDS. *Intensive Care Med*. 2010;36(6):963–970. doi:10.1007/s00134-010-1851-3
6. Mowery NT, Terzian WH, Nelson AC. Acute lung injury. *Curr Probl Surg*. 2020;57(5):100777. doi:10.1016/j.cpsurg.2020.100777
7. Jesús V, Carlos F, Domingo M, et al. Dexamethasone treatment for the acute respiratory distress syndrome: a multicentre, randomised controlled trial. *Lancet Respir Med*. 2020;8(3):267–276. doi:10.1016/s2213-2600(19)30417-5
8. Rong C, Chen C, Huimin L, et al. Macrophage Sprouty4 deficiency diminishes sepsis-induced acute lung injury in mice. *Redox Biol*. 2022;58:102513. doi:10.1016/j.redox.2022.102513
9. Patel VJ, Biswas Roy S, Mehta HJ, Joo M, Sadikot RT. Alternative and natural therapies for acute lung injury and acute respiratory distress syndrome. *BioMed Res Int*. 2018;2018:2476824. doi:10.1155/2018/2476824
10. Yinpin D. The applied value analysis of Tingli Dazao Xiefei decoction and Sanzi yangqin decoction on pulmonary heart disease. *Cardiovasc Dis Electron J Integr Tradit Chin West Med*. 2019;7(17):147–148. Chinese. doi:10.16282/j.cnki.cn11-9336/r.2019.17.120
11. Min X. Efficacy of the Tingli Dazao Xiefei decoction on ARDS caused by pulmonary contusion. *Clin J Chin Med*. 2018;10(8):19–21. Chinese. doi:10.3969/j.issn.1674-7860.2018.08.008
12. Wenjing W. Effect of tingli dazao xiefei decoction on pulmonary function and inflammation in patients with lung abscess. *Guangming J Chin Med*. 2022;37(19):3533–3535. Chinese. doi:10.3969/j.issn.1003-8914.2022.19.024
13. Kelei S, Xingjiang X. Treatment strategy and thought on classical herbal formulae for coronavirus disease 2019. *Chin J Chin Mater Med*. 2021;46(2):494–503. doi:10.19540/j.cnki.cjcmm.20200603.501
14. Xu L, Yan C, Xuesong B, et al. Research progress on the mechanism of traditional Chinese medicine treatment of acute lung injury / acute respiratory distress syndrome. *J Liaoning Univ Tradit Chin Med*. 2017;19(1):166–170. Chinese. doi:10.13194/j.issn.1673-842x.2017.01.049
15. Jinghua L, Wangxiao T, Siwei W, Yu W, Xiaoying W. Study on the mechanism of Tingli Dazao Xiefei decoction in the treatment of COVID-19 based on the network pharmacology. *Shandong Sci*. 2020;33(5):1–13. Chinese. doi:10.3976/j.issn.1002-4026.2020.05.001
16. Liang L, Lina W, Lei W, et al. Mechanism action of Tingli Dazao Xiefei Tang in the treatment of children with pneumonia based on network pharmacology. *J Pediatr Tradit Chin Med*. 2021;17(1):8–13. Chinese. doi:10.16840/j.issn1673-4297.2021.01.03
17. Qian L, Fengxia S, Yun M, et al. Based on network pharmacology and molecular docking technology to explore the mechanism of tingli dazao xiefei decoction in the treatment of chronic pulmonary heart disease. *Res Pract Chin Med*. 2021;35(06):33–39. Chinese. doi:10.13728/j.1673-6427.2021.06.008
18. Jiaqi Y, Yifan M, Yumei Z, et al. Dao-chi powder ameliorates pancreatitis-induced intestinal and cardiac injuries via regulating the Nrf2-HO-1-HMGB1 signaling pathway in rats. *Front Pharmacol*. 2022;13:922130. doi:10.3389/fphar.2022.922130
19. Jinlong R, Peng L, Jinan W, et al. TCMSP: a database of systems pharmacology for drug discovery from herbal medicines. *J Cheminf*. 2014;6(13):6. 13. doi:10.1186/1758-2946-6-13
20. Zhongyang L, Feifei G, Yong W, et al. BATMAN-TCM: a bioinformatics analysis tool for molecular mechANism of Traditional Chinese medicine. *Sci Rep*. 2016;6:21146. doi:10.1038/srep21146
21. Fan Y. Canker sores in the lungs. In: *Medical Treasures of the Golden Chamber*. Chin press Tradit Chin Med; 2003:117.
22. Xinguo W. Basic knowledge of pharmacological experimental design in Chinese medicine. In: *Pharmacology of Chinese Medicine Experimental Course*. Chin press Tradit Chin Med; 2017:8.
23. Yuan R, Peipei Y, Panying L, et al. Tingli Dazao Xiefei Decoction ameliorates asthma in vivo and in vitro from lung to intestine by modifying NO–CO metabolic disorder mediated inflammation, immune imbalance, cellular barrier damage, oxidative stress and intestinal bacterial disorders. *J Ethnopharmacol*. 2023;313:116503. doi:10.1016/j.jep.2023.116503
24. Beibei Z, Mengnan Z, Qinqin Z, et al. Effects of Tingli Dazao Xiefei decoction on the immune inflammation and intestinal flora in asthmatic rats. *Acta Pharm Sin*. 2022;57(8):2364–2377. Chinese. doi:10.16438/j.0513-4870.2022-0116
25. Nolan T, Hands RE, Bustin SA. Quantification of mRNA using real-time RT-PCR. *Nat Protoc*. 2006;1(3):1559–1582. doi:10.1038/nprot.2006.236
26. Xiaoqian L, Cong S, Zhonghua W, Hongji Y, Aidong Y, Bo T. Emodin alleviated pulmonary inflammation in rats with LPS-induced acute lung injury through inhibiting the mTOR/HIF-1 alpha/VEGF signaling pathway. *Inflamm Res*. 2020;69(4):365–373. doi:10.1007/s00011-020-01331-3
27. Hongxia Z. Clinical observation on wuhu decoction combined with Tingli Dazao Xiefei decoction in treating mycoplasma pneumonia in children of phlegm-heatobstructing the lung type. *Pract Clin J Integr Tradit Chin West Med*. 2021;21(13):104–105. Chinese. doi:10.13638/j.issn.1671-4040.2021.13.051
28. Lian L, Jiangbo T, Weijun H, Yang L. Clinical observation on wuhu decoction combined with Tingli Dazao Xiefei decoction in treating bronchial pneumonia in children of phlegm-heatobstructing the lung type. *Chin Med Mod Distance Educ Chin*. 2022;20(16):96–98. Chinese. doi:10.3969/j.issn.1672-2779.2022.16.036
29. Xiaohui X. Efficacy of modified Tingli Dazao Xiefei decoction in treating bronchial asthma and evaluation of patients' adverse reactions. *Contemp Med*. 2022;28(6):7–10. Chinese. doi:10.3969/j.issn.1009-4393.2022.06.003
30. Yufeng S, Fanxiao K, Chunsheng F. Efficacy observation of modified Zhenwu Decoction and Tingli Dazao Xiefei Decoction on pneumoconiosis. *Chin J Mod Drug Appl*. 2022;16(12):147–150. Chinese. doi:10.14164/j.cnki.cn11-5581/r.2022.12.048
31. Kejing Y, Zhixin Q. Clinical observation on treatment of acute respiratory distress syndrome caused by lung contusion with modified Tingli Dazao Xiefei decoction. *J Emerg Tradit Chin Med*. 2016;25(5):878–880. Chinese. doi:10.3969/j.issn.1673-7202.2016.09.016

32. Qin MZ, Qin MB, Liang ZH, Tang GD. Effect of SOCS3 on lung injury in rats with severe acute pancreatitis through regulating JAK2/STAT3 signaling pathway. *Riv Eur Sci Med Farmacol*. 2019;23(22):10123–10131. doi:10.26355/eurrev_201911_19582
33. Xiao H, Yuxi W, Hailong C, et al. Enhancement of ICAM-1 via the JAK2/STAT3 signaling pathway in a rat model of severe acute pancreatitis-associated lung injury. *Exp Ther Med*. 2016;11(3):788–796. doi:10.3892/etm.2016.2988
34. Caixia L, Yuhong L, Han Z, et al. Xuanfei Baidu Decoction suppresses complement overactivation and ameliorates IgG immune complex-induced acute lung injury by inhibiting JAK2/STAT3/SOCS3 and NF-Kappa B signaling pathway. *Phytomedicine*. 2023;109:154551. doi:10.1016/j.phymed.2022.154551
35. Shuiqiao F, Weina L, Wenqia Y, Jun H. Protective effect of Cordyceps sinensis extract on lipopolysaccharide-induced acute lung injury in mice. *Biosci Rep*. 2019;39(6):Bsr20190789. doi:10.1042/bsr20190789
36. Huahe Z, Shun W, Cong S, et al. Mechanism of protective effect of xuan-bai-cheng-qi decoction on LPS-induced acute lung injury based on an integrated network pharmacology and RNA-sequencing approach. *Respir Res*. 2021;22(1):188. doi:10.1186/s12931-021-01781-1
37. Yanru W, Xiaojie J, Qin F, et al. Deciphering the active compounds and mechanisms of HSBDF for Treating ALI via integrating chemical bioinformatics analysis. *Front Pharmacol*. 2022;13:879268. doi:10.3389/fphar.2022.879268
38. Daxue H, Shengquan W, Gaofeng F, et al. LXRs/ABCA1 activation contribute to the anti-inflammatory role of phytosterols on LPS-induced acute lung injury. *J Funct Foods*. 2022;89:104966. doi:10.1016/j.jff.2022.104966
39. Ruihua Z, Xia A, Yongjie D, et al. Kaempferol ameliorates H9N2 swine influenza virus-induced acute lung injury by inactivation of TLR4/MyD88-mediated NF-kappa B and MAPK signaling pathways. *Biomed Pharmacother*. 2017;89:660–672. doi:10.1016/j.biopha.2017.02.081